THE JOURNAL OF BIOLOGICAL CHEMISTRY VOL. 288, NO. 52, pp. 37308–37318, December 27, 2013
© 2013 by The American Society for Biochemistry and Molecular Biology, Inc. Published in the U.S.A.

Bioengineered Chinese Hamster Ovary Cells with Golgi-targeted 3-*O*-Sulfotransferase-1 Biosynthesize Heparan Sulfate with an Antithrombin-binding Site*

Received for publication, September 16, 2013, and in revised form, November 2, 2013 Published, JBC Papers in Press, November 18, 2013, DOI 10.1074/jbc.M113.519033

Payel Datta[‡§], Guoyun Li[§¶‖], Bo Yang[§¶], Xue Zhao[‖], Jong Youn Baik[**], Trent R. Gemmill[**], Susan T. Sharfstein[**], and Robert J. Linhardt[‡§¶‡‡1]

*From the Departments of [‡]Biology, [§]Chemistry and Chemical Biology, and [‡‡]Chemical and Biological Engineering and the [¶]Center for Biotechnology and Interdisciplinary Studies, Rensselaer Polytechnic Institute, Troy, New York 12180, the [‖]College of Food Science and Technology, Ocean University of China, Qingdao 266003, China, and the **SUNY College of Nanoscale Science and Engineering, Albany, New York 12203*

Background: CHO-S cells produce non-anticoagulant heparan sulfate (HS) even when transfected with HS3st1 and NDST2.
Results: Golgi targeting of HS3st1 alone in bioengineered CHO-S cells afforded anticoagulant HS.
Conclusion: Targeting of HS3st1 to the Golgi ensured its action in biosynthesis and modified the action of other biosynthetic enzymes.
Significance: Engineering the production of HS and potentially heparin could provide a safer form of this important anticoagulant drug.

HS3st1 (heparan sulfate 3-*O*-sulfotransferase isoform-1) is a critical enzyme involved in the biosynthesis of the antithrombin III (AT)-binding site in the biopharmaceutical drug heparin. Heparin is a highly sulfated glycosaminoglycan that shares a common biosynthetic pathway with heparan sulfate (HS). Although only granulated cells, such as mast cells, biosynthesize heparin, all animal cells are capable of biosynthesizing HS. As part of an effort to bioengineer CHO cells to produce heparin, we previously showed that the introduction of both *HS3st1* and *NDST2* (*N*-deacetylase/*N*-sulfotransferase isoform-2) afforded HS with a very low level of anticoagulant activity. This study demonstrated that untargeted HS3st1 is broadly distributed throughout CHO cells and forms no detectable AT-binding sites, whereas Golgi-targeted HS3st1 localizes in the Golgi and results in the formation of a single type of AT-binding site and high anti-factor Xa activity (137 ± 36 units/mg). Moreover, stable overexpression of HS3st1 also results in up-regulation of 2-*O*-, 6-*O*-, and *N*-sulfo group-containing disaccharides, further emphasizing a previously unknown concerted interplay between the HS biosynthetic enzymes and suggesting the need to control the expression level of all of the biosynthetic enzymes to produce heparin in CHO cells.

Heparan sulfate (HS)[2] glycosaminoglycans (GAGs) are involved in many cellular functions, including cell signaling cascades, embryonic development, and blood coagulation, and in viral/bacterial infections (1). Heparin is a highly sulfated form of HS GAG. Heparin and low molecular weight heparin are widely utilized as biopharmaceutical drugs for acute care and short-term anticoagulant therapy, including cardiac bypass, hemodialysis, and deep vein thrombosis. More than 100 tons of heparin are used annually, with a market value of approximately $7 billion (2). Understanding the rate-limiting factors that govern HS and heparin biosynthesis is critical for production of heparin-based drugs from non-animal sources.

HS and heparin are biosynthesized in the Golgi of animal cells in three main steps involving chain initiation, polymerization, and modification (3, 4). Initiation of GAG biosynthesis begins with the addition of a tetrasaccharide linker (–GlcUAβ1→3Galβ1→3Galβ1→4Xylβ1→*O*-Ser) on specific serine residues of a core protein (5–7). In the case of heparin, only serglycin is modified with heparin GAG chains (8), whereas HS can be found on a number of different core proteins, most typically members of the syndecan and glypican families (9). Polymerization of HS (and heparin) occurs by action of EXT1 and EXT2 enzymes, with sequential attachment of GlcUA and GlcNAc residues to form a linear GlcUAβ1→4GlcNAcα1→4 homocopolymer called heparosan (10). The heparosan chain undergoes a series of modification steps including (i) *N*-deacetylation and *N*-sulfonation of GlcNAc to form GlcNS through action of *N*-deacetylase/*N*-sulfotransferase (NDST1–4) (11–18), (ii) epimerization of glucuronic acid to form iduronic acid by action of C5-epimerases (GLCE) (19), (iii) 2-*O*-sulfonation at C2 of iduronic acid and glucuronic acid by 2-*O*-sulfotransferase (HS2st) (20), (iv) 6-*O*-sulfonation of glucosamine by 6-*O*-sulfotransferases (HS6st1–3) (21–24), and (v) 3-*O*-sulfonation of glucosamine through action of 3-*O*-sulfotransferases (HS3st1–7) (25–27). Most of the sulfotransferases have tissue-specific isoforms, and the action of the isoforms affords tissue-specific

* This work was supported, in whole or in part, by National Institutes of Health Grant R01 GM090127. This work was also supported by a fellowship from the Rensselaer Polytechnic Institute (to P. D.).
[1] To whom correspondence should be addressed: Center for Biotechnology and Interdisciplinary Studies, Rensselaer Polytechnic Institute, Troy, NY 12180. Tel.: 518-276-3404; Fax: 518-276-3405; E-mail: linhar@rpi.edu.
[2] The abbreviations used are: HS, heparan sulfate; GAG, glycosaminoglycan; GLCE, glucuronyl C5-epimerase; AT, antithrombin III; CS/DS, chondroitin sulfate/dermatan sulfate; AMAC, 2-aminoacridine; PAPS, 3′-phosphoadenosine 5′-phosphosulfate.

Downloaded from http://www.jbc.org/ at RENSSELAER POLYTECHNIC IN on December 30, 2013

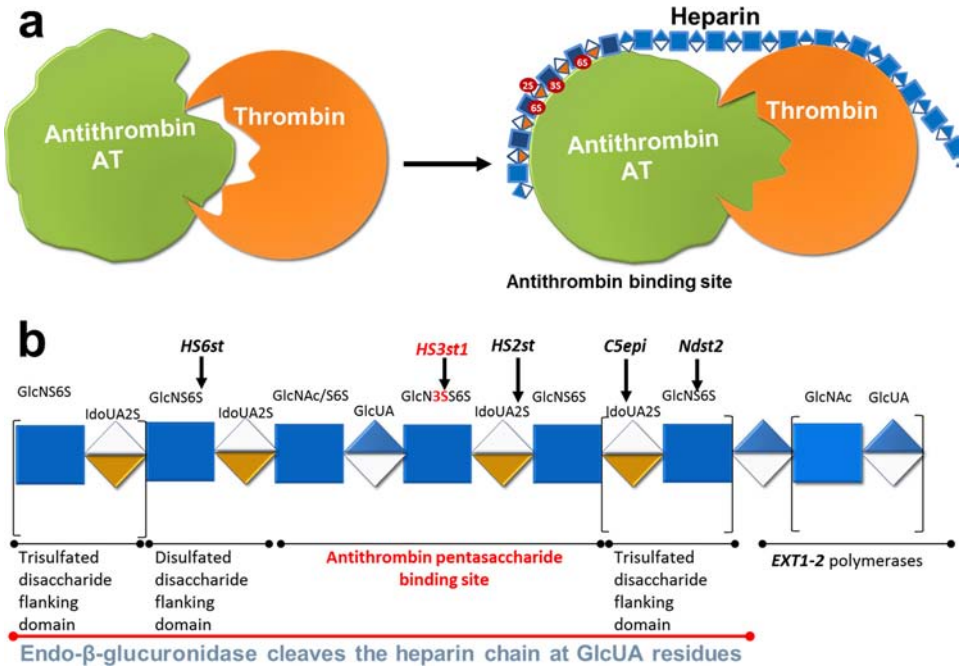

FIGURE 1. **Anticoagulant heparin.** *a*, mode of action of heparin. During the blood coagulation cascade, serine proteases are activated, resulting in activation of prothrombin to form thrombin and causing blood clot formation. Heparin catalyzes the binding of AT and thrombin, resulting in increased efficacy of the AT-thrombin interaction and decreased clot formation. *b*, biosynthesis of anticoagulant heparin. The critical steps in heparin biosynthesis involve the concerted action of *N*-sulfonation (NDST2), epimerization (GLCE), 6-*O*-sulfonation (6-sulfotransferases, HS6sts), and, finally, GAG chain modification by 3-*O*-sulfonation (HS3st1). Anticoagulant heparin is characterized by AT pentasaccharide-binding sites. *IdoA*, IdoUA; *GlcA*, GlcUA; *C5epi*, C5-epimerase.

sulfated domains on HS (3, 4, 28). Partially sulfated domains in HS can result in specific ligand binding characteristic to HS. Completely or nearly completely sulfated domains in HS (and heparin) are usually characterized as containing antithrombin III (AT)-binding sites and anticoagulant activity. The AT-binding sites interact with the serine protease inhibitor AT, causing it to undergo a conformational change and increasing the ability of AT to inhibit thrombin and factor Xa, resulting in anticoagulation (see Fig. 1*a*). Pharmaceutical heparin is commonly isolated and purified from pig or cow mucosal tissues rich in mast cells. Concerns over the contamination or adulteration of animal-sourced heparins motivate our efforts to produce heparin from non-animal sources (2).

Production of heparin from non-animal sources will require understanding the control and interplay of heparin/HS biosynthetic enzymes. Heparin is naturally produced in serous and connective tissue mast cells (29), and mast cell maturation is accompanied by an increase in heparin/HS biosynthetic enzymes (8). Heparin biosynthesis initiates on the serglycin core protein, followed by chain elongation and chain modification. In addition, the heparin chain is cleaved by a β-endoglucuronidase called heparanase (3). The critical steps in heparin biosynthesis involve (i) the action of NDST2 (15, 17, 30), (ii) the action of GLCE (31), (iii) 6-*O*-sulfonation by HS6st1 and HS6st2 (32, 33), and (iv) GAG chain modification by HS3st1 (34, 35) (Fig. 1*b*). There could also be additional factors that aid in the production of heparin in mast cells, including the optimal expression and localization of biosynthetic enzymes, appropriate core protein biosynthesis, and the presence of as yet undiscovered biosynthetic chaperones.

CHO have been widely utilized for the production of biopharmaceuticals (36) and exhibit most of the biosynthetic machinery required to prepare HS and heparin (37, 38). We previously demonstrated that a suspension-adapted CHO cell line (CHO-S) expressing endogenous HS biosynthetic enzymes (NDST1, GLCE, HS2st, and HS6sts) could be sequentially bioengineered to stably overexpress exogenous human NDST2 and mouse HS3st1 (39). This resulted in bioengineered CHO-S cells (40 CHO-S dual clones with varied expression of NDST2 and HS3st1) that expressed HS with a very low level of anticoagulant activity but rich in *N*-sulfo groups (39). The results of this previous study suggest that overexpression of *NDST2* may overmodify the HS chain, forming so many *N*-sulfoglucosamine residues that HS3st1 might have no available substrate upon which to act. Alternatively, there may be a limitation of sulfate and/or a decreased activity or mislocalization of HS3st1. These questions led us to probe factors that might impact HS3st1 activity in bioengineered CHO-S cells.

EXPERIMENTAL PROCEDURES

Cell Lines and Cell Culture—CHO-S cells (Invitrogen) and stable recombinant CHO-S dual clones (Dual-10, Dual-3, Dual-20, Dual-22, and Dual-29) were cultured in CD CHO medium (Invitrogen) supplemented with 8 mM GlutaMAX™ (Invitrogen) and 2% hypoxanthine thymidine solution. Dual clones were routinely kept under selective pressure of 1 mg/ml G418 and 500 μg/ml Zeocin. Cells were seeded at 2×10^5 cells/ml in 125-ml polycarbonate Erlenmeyer flasks (Corning, Corning, NY) and cultured on orbital shakers (125 rpm) in a humidified 37 °C incubator at 5% CO_2.

Cloning and Expression of Golgi-targeted HS3st1—The pTagRFP-Golgi expression vector (Evrogen) encodes the red fluorescent protein TagRFP fused to a Golgi-targeting sequence (fragment of human β1→4-galactosyltransferase). pGTS-HS3st1

Downloaded from http://www.jbc.org/ at RENSSELAER POLYTECHNIC IN on December 30, 2013

was created using the pTagRFP-Golgi expression vector by deleting the red fluorescent protein gene and inserting the gene encoding mouse HS3st1 (GenBank™ accession number BC009133.1; Thermo Fisher Scientific). Mouse *Hs3st1* was amplified using a forward primer including an AgeI restriction site (5′-CAAGGATCCACCGGTCGCCACCCACCCGGCTGCTCCT-GGC-3′) and a reverse primer including a NotI restriction site (5′-GGCAGAACATTCGACTGGCACTGAGCGGCCGCGA-CTCTAG-3′) and inserted into a pTag-Golgi expression vector.

Bulk Pool Transfection of CHO-S Cells with Golgi-targeted HS3st1 Expression Vector—The pGTS-HS3st1 expression vector was used for transfecting CHO-S cells with a 4D-Nucleofector® system (Kit-SG, program FF137; Lonza, Basel, Switzerland) according to the manufacturer's instructions. The transfected cells were cultured in CD CHO medium supplemented with 8 mM GlutaMAX™ and 2% hypoxanthine thymidine solution. 48 h post-transfection, the cells were treated with 1 mg/ml G418 for 3–4 weeks to form a bulk stable transfectant pool. The bulk pool transfection was performed on two separate occasions to generate independent bulk stable pools for analysis of HS composition and function.

Transient Transfection of CHO-S Cells with EXT1/2 Expression Vectors—The EXT1, EXT2, and EXT1/2 expression vectors (graciously provided by Dr. Lena Kjellén, Uppsala University, Uppsala, Sweden) (40) were used for transfecting CHO-S cells using the 4D-Nucleofector® system according to the manufacturer's instructions. The transfected cells were cultured in CD CHO medium supplemented with 8 mM GlutaMAX™ and 2% hypoxanthine thymidine solution. 36 h post-transfection, the HS composition of the cells was analyzed.

Localization of Heparin/HS Modification Enzymes—Cells were washed with sterile Dulbecco's PBS and fixed with 4% paraformaldehyde for 15 min at room temperature. Cells were permeabilized with permeabilization buffer (Invitrogen), 10% FBS, and Dulbecco's PBS for 10 min. Cells were stained with rabbit anti-NDST2 (AP5759B, Abgent), rabbit anti-HS3st1 (ab91065, Abcam), rabbit anti-HS2st1 (ab108541, Abcam), and goat anti-GM130 Golgi marker (ab1299, Abcam) primary antibodies following the manufacturers' instructions overnight at 4 °C in the dark. Cells were washed once and stained with Alexa Fluor 647-conjugated donkey anti-rabbit IgG and Alexa Fluor 488-conjugated donkey anti-goat IgG secondary antibodies (Molecular Probes) following the manufacturer's instructions. Cells were mounted onto glass slides with ProLong Gold and DAPI (Invitrogen). Imaging was performed using an inverted Zeiss LSM 510 laser scanning confocal microscope equipped with a META detector. Dual-29 cells were used as a positive control, and the other cell samples were then evaluated at the same frequency. Images were acquired and processed using Zeiss LSM image browser software. For imaging, signal intensities were adjusted for Dual-29 cells, and other cells were imaged at the same configurations.

Disaccharide Analysis—Cells and spent media were proteolyzed with Actinase E solution, and GAGs were purified using a strong anion exchange spin column, released with salt, and alcohol-precipitated as described previously (41). Complete depolymerization of the GAGs was performed using polysaccharides lyases. A mixture of heparin/HS lyases I, II, and III (10 milliunits each) in 5 μl of 25 mM Tris, 500 mM NaCl, and 300 mM imidazole buffer (pH 7.4) was added and incubated at 35 °C for 10 h to depolymerize heparin/HS GAGs. The heparin/HS disaccharides were recovered by centrifugal filtration using a YM-10 spin column, and the disaccharides were collected in the flow-through and lyophilized.

The HS disaccharide standards had the following structures: ΔUA(1→4)GlcNAc (0S), ΔUA2S(1→4)GlcNAc (2S), ΔUA(1→4)GlcNcA6S (6S), ΔUA2S(1→4)GlcNAc6S (2S6S), ΔUA(1→4)GlcNS (NS), ΔUA2S(1→4)GlcNS (NS2S), ΔUA(1→4)GlcNS6S (NS6S), and ΔUA2S(1→4)GlcNS6S (TriS), where ΔUA is 4-deoxy-α-L-*threo*-lex-4-enopyranosyluronic acid, GlcN is glucosamine, S is sulfo, and Ac is acetyl. Chondroitin sulfate/dermatan sulfate (CS/DS) disaccharide standards had the following structures: ΔUA(1→3)GalNAc (0S), ΔUA(1→3)GalNAc6S (6S), ΔUA(1→3)GalNAc4S (4S), ΔUA2S(1→3)GalNAc (2S), ΔUA(1→3)GalNAc4S6S (SE), ΔUA2S(1→3)GalNAc6S (SD), ΔUA2S(1→3)GalNAc4S (SB), and ΔUA2S(1→3)GalNAc4S6S (TriS), where GalN is galactosamine. The HA disaccharide standard had the structure ΔUA(1→3)GlcNAc. All disaccharide standards were from Iduron Ltd. (Manchester, United Kingdom).

Derivatization of unsaturated disaccharides with 2-aminoacridine (AMAC) was performed. The freeze-dried biological sample containing GAG-derived disaccharides (~5 μg) or a mixture of eight heparin/HS disaccharide standards (5 μg/each disaccharide) was added to 10 μl of 0.1 M AMAC solution in acetic acid/dimethyl sulfoxide (3:17, v/v) and mixed by vortexing for 5 min. Next, 10 μl of 1 M $NaBH_3CN$ was added in the reaction mixture and incubated at 45 °C for 4 h. Finally, the AMAC-tagged disaccharide mixtures were diluted to different concentrations (0.5–100 ng) using 50% (v/v) aqueous dimethyl sulfoxide, and AMAC/LC-MS analysis was performed.

LC-MS analyses were performed on an Agilent 1200 LC/MSD instrument equipped with a 6300 ion trap and a binary pump. An Agilent Poroshell 120 C_{18} column (3.0 × 150 mm, 2.7 μm) was used at 45 °C. Eluant A was 80 mM ammonium acetate solution, and eluant B was methanol. Eluant A and 15% eluant B was flowed (150 μl/min) through the column for 5 min, followed by linear gradients of 15–30% eluant B from 5–30 min. The column effluent entered the electrospray ionization MS source for continuous detection by MS. The electrospray interface was set in negative ionization mode with a skimmer potential of −40.0 V, a capillary exit of −40.0 V, and a source temperature of 350 °C to obtain the maximum abundance of the ions in a full-scan spectrum (300–1200 Da). Nitrogen (8 liters/min, 40 p.s.i.) was used as a drying and nebulizing gas.

Tetrasaccharide Analysis—GAGs were isolated from cells and spent media; treated with heparin lyase-2 (10 milliunits) in 5 μl of 25 mM Tris, 500 mM NaCl, and 300 mM imidazole buffer (pH 7.4); and incubated at 35 °C for 10 h to depolymerize heparin/HS GAGs. The depolymerized products were recovered by centrifugal filtration using a YM-10 spin column, collected in the flow-through, and lyophilized.

An Agilent Poroshell 120 C_{18} column (2.1 × 100 mm, 2.7 μm) was used at 45 °C. Eluant A was water/acetonitrile (85:15, v/v), and eluant B was water/acetonitrile (35:65, v/v). Both eluants contained 12 mM tributylamine and 38 mM ammonium

Downloaded from http://www.jbc.org/ at RENSSELAER POLYTECHNIC IN on December 30, 2013

acetate with the pH adjusted to 6.5 with acetic acid. A gradient of eluant A for 2 min followed by a linear gradient of 0–30% eluant B for 2–40 min was used at flow rate of 120 μl/min. The column effluent entered the electrospray ionization MS source for continuous detection by MS. The electrospray interface was set in negative ionization mode with a skimmer potential of −40.0 V, a capillary exit of −40.0 V, and a source temperature of 350 °C to obtain the maximum abundance of the ions in a full-scan spectrum (300–1500 Da). Nitrogen (8 liters/min, 40 p.s.i.) was used as a drying and nebulizing gas.

Fractionation of GAGs by Strong Anion Exchange Chromatography—Fractionation of heparin/HS GAGs was performed using a mini strong ion exchange column to quantitate the amounts of less sulfated HS and highly sulfated heparin/HS (42). Briefly, cells were proteolyzed with Actinase E solution. CS/DS GAGs were isolated from total GAGs, and the less sulfated HS fraction was purified using a strong anion exchange spin column, released by washing the column three times with 300 μl of 0.5 M NaCl, and alcohol-precipitated. The heparin/HS fractions were released by washing the column three times with 300 μl of 1.6 M NaCl, followed by alcohol precipitation. Purified GAGS were quantified using AMAC/LC-MS and/or carbazole assay as described previously (41).

Anticoagulant Activity Analysis of Bioengineered HS by Anti-factor Xa Assay—The anti-factor Xa anticoagulation activity assay was performed with a heparin anti-factor Xa assay kit (HemosIL™, Instrumentation Laboratory, Bedford, MA). The chromogenic substrate Arg-Gly-Arg-*p*-nitroanilide was either from the HemosIL heparin kit or from Hyphen BioMed (Neuville-sur-Oise, France). Tris, NaCl, and heparin (Sigma) were reagent-grade or better.

In brief, 100-μl reactions in TBS (0.9% NaCl and 50 mM Tris (pH 8.4)) containing 5 μl (5 mIU) of antithrombin solution, 2 μl (0.0272 nanokatals) of factor Xa solution, and the purified GAG or standard heparin samples (at various concentrations) were covered in a 96-well plate (Costar) and incubated for 1 h on a rocking platform. Next, 20 μl of a 0.75 mg/ml solution of the chromogenic substrate in TBS was added to each well. The rate of hydrolysis of the substrate was monitored by measuring the absorbance at 410 nm over the course of 1 h in a Tecan Infinite M200 plate reader operating at the maximum sampling rate. The rate curves were linearized by taking into account the decreasing substrate concentration as the reaction progressed. The concentrations of standard heparin samples were then plotted against the reciprocal of their rates of hydrolysis, and the slope was used to determine analyte concentrations. Statistical analysis was performed by comparison with Student's *t* test ($n = 3$).

Quantification of AT and FGF-2 Binding by Flow Cytometry—AT and FGF-2 were labeled with amine-reactive BODIPY® R6G SE (4,4-difluoro-5-phenyl-4-bora-3,4*a*-diaza-*s*-indacene-3-propionic acid succinimidyl ester, Invitrogen) (39). In brief, BODIPY R6G solution (10 μl) was added to the AT or FGF-2 solution (1 mg of AT or FGF-2 in 100 ml of 0.1 M sodium bicarbonate buffer), and the reaction mixtures were incubated in the dark at 37 °C for 1 h with continuous stirring. The reactions were stopped by adding 1 ml of sterile PBS and purified with M_r 3000 cutoff spin columns (Millipore, Bedford, MA). Concentrated BODIPY R6G-conjugated FGF-2 or AT was diluted in 1 ml of PBS containing 10% FBS and stored at −20 °C for up to 14 days until used directly for labeling cells.

Flow cytometry experiments were performed with BODIPY R6G-conjugated AT or FGF-2. Briefly, 10^6 exponentially growing cells were washed with cold sterile Dulbecco's PBS containing 10% FBS. The cells were incubated with BODIPY R6G-conjugated AT or FGF-2 for 30 min at 4 °C in the dark. The cells were washed with cold sterile Dulbecco's PBS containing 10% FBS. The cells were fixed with freshly prepared 4% paraformaldehyde and analyzed. A minimum of 10,000 cells from each sample was analyzed on a BD LSR II flow cytometer with FITC excitation filters (530 nm; BD Biosciences). A 488-nm argon ion laser was used for excitation, and a 530/30-nm band pass emission filter was used to detect fluorescence.

RESULTS AND DISCUSSION

Pharmaceutical heparin characteristically has a varied disaccharide composition, composed of seven to eight different disaccharides and dominated by a preponderance of TriS (43, 44). In contrast, CHO-S cells produce HS with a simpler structure, primarily composed of the *N*-acetylated 0S disaccharide with smaller amounts of NS as well as minor amounts of disaccharides containing *O*-sulfo groups. The bioengineering of CHO-S cells to produce heparin requires decreasing *N*-acetyl-containing disaccharides from 80 to 10% and increasing the *N*-sulfo group-containing disaccharides from 20 to 90% while enhancing the level of *O*-sulfo groups and increasing structural diversity. Thus, a balancing of the activities of the required biosynthetic enzymes is critical in the bioengineering of CHO-S cells to prepare heparin.

Structure, expression, localization, and substrate availability are crucial for the proper activity of biosynthetic enzymes. The incorporation of sulfo groups into HS occurs within the Golgi. With the exception of HS3sts, all of the HS modification enzymes, including NDSTs, GLCE, HS2st, and HS6sts, have transmembrane domains causing them to localize within the Golgi (3). HS3st1 is crucial for generating the AT-binding site in both HS and heparin. Indeed, mice deficient in HS3st1 lack anticoagulant heparin production in their mast cells (34, 35), yet HS3st1 is a soluble Golgi-resident protein with a small transmembrane domain.

In our previous study, CHO-S cells were stably transfected with human *NDST2* and mouse *Hs3st1* (to produce 40 dual expression clones) (Fig. 2*a*), and the expression levels of HS3st1 and NDST2 were evaluated (39). Characterization of two dual clones, Dual-29 and Dual-3, showed an HS with a high percentage of *N*-sulfo group-containing disaccharide residues (39). In this study, we began by screening the disaccharide composition of HS produced in the dual clones from cell pellets (Fig. 2*b*) and spent media (data not shown). In parallel, the expression and localization of NDST2 and HS3st1 were evaluated (Fig. 3). The parent CHO-S cells showed no detectable HS3st1 and NDST2 (Fig. 3), and the HS disaccharide composition was dominated by unsulfated disaccharides (0S) (Fig. 2*b*). Screening of dual clones that express variable levels of HS3st1 and NDST2 showed that the bioengineered HS composition was dominated by NS, in conjunction with diverse ratios of NS, NS2S, and 0S

Downloaded from http://www.jbc.org/ at RENSSELAER POLYTECHNIC IN on December 30, 2013

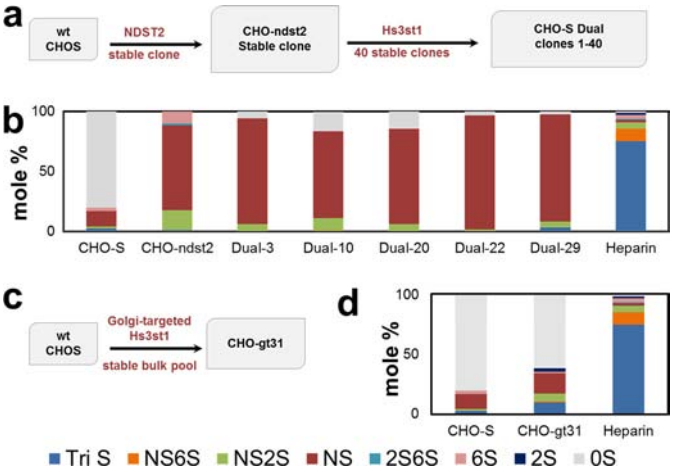

FIGURE 2. **CHO-S dual clones demonstrate highly *N*-sulfated heparin/HS.** *a*, metabolic engineering strategy showing that CHO-S cells were first bioengineered to stably overexpress NDST2 before being stably transfected with HS3st1 to prepare 40 stable dual clones. *b*, HS disaccharide composition analysis performed on GAGs isolated from CHO-S, CHO-ndst2, and dual clones. Heparin/HS disaccharide composition analysis was performed on GAGs isolated from the cell pellet. All of the dual clones showed highly *N*-sulfated HS. Expression of NDST2 and HS3st1 varied among the selected clones (Dual-3, Dual-10, Dual-20, Dual-22, and Dual-29). *c*, metabolic engineering strategy showing CHO-S cells stably transfected with Golgi-targeted HS3st1 plasmid. *d*, HS disaccharide composition analysis performed on GAGs isolated from parental CHO-S and CHO-gt31 cell pellets. CHO-gt31 cells demonstrated an increase in TriS. HS disaccharide analysis was performed by AMAC/LC-MS. Heparin was used as a positive control.

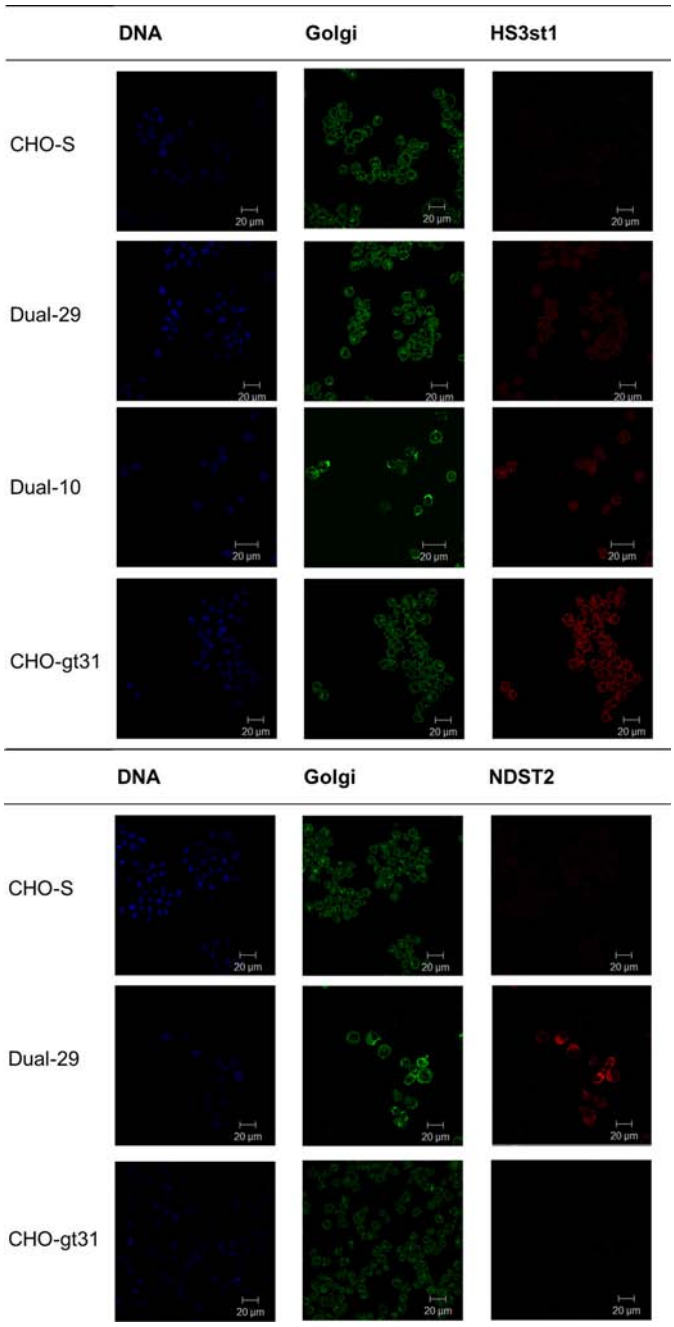

FIGURE 3. **Expression and localization of HS3st1 and NDST2 in CHO-S, Dual-29, Dual-10, and CHO-gt31 cells.** Overexpression of HS3st1 in Dual-29 cells resulted in a broad distribution of HS3st1. Overexpression of HS3st1 in Dual-10 cells localized HS3st1 in the Golgi. Overexpression of Golgi-targeted HS3st1 in CHO-gt31 localized HS3st1 in the Golgi. NDST2 was localized in the Golgi. DAPI was used to visualize nuclei, and anti-GM130 Golgi marker antibodies were used to stain the Golgi compartment. Colocalization experiments were performed using confocal microscopy. Dual-29 cells were used as the positive control. For imaging, signal intensities were adjusted for Dual-29 cells, and other cells were imaged at the same frequencies and configurations.

disaccharides (Fig. 2*b*). In Dual-29 cells, which express a high level of HS3st1 and NDST2, HS3st1 showed a broad distribution (Fig. 3); however, NDST2 was localized in the Golgi (Fig. 3). The disaccharide composition of Dual-29 cells also included TriS in addition to the NS, NS2S, and 0S observed in all of the dual clones. In contrast, in Dual-10 cells, which express a lower level of HS3st1, HS3st1 was correctly localized to the Golgi (Fig. 3) and contained the highest level of 0S. All of the dual clones afforded an HS that was much higher in NS disaccharide content compared with the parent CHO-S cell HS or heparin (Fig. 2*b*).

Expression of Golgi-targeted HS3ST1 in CHO-S Cells Results in Remodeling of the Proteoglycanome of Bioengineered CHO-gt31 Cells—Because of the variability of the individual dual clones, bulk pool stable CHO-S cell transfectants with Golgi-targeted HS3st1 were created to ensure the correct localization of HS3st1 (Fig. 2, *c* and *d*). These CHO-gt31 cells showed Golgi-localized expression of HS3st1 but no detectable expression of NDST2 compared with Dual-29 cells (Fig. 3).

HS GAGs were isolated and purified from CHO-S, CHO-ndst2, Dual-29, and CHO-gt31 cell lines and subjected to disaccharide composition analysis by AMAC/LC-MS. Because of the absence of detectable NDST2, the HS from the CHO-gt31 cells had a disaccharide composition with considerably less *N*-sulfo group-containing disaccharides (~40%) than either the NDST2 stable clone or any of the dual transfectants (Fig. 2*d*). The HS from the CHO-gt31 cells was more varied in disaccharide composition, composed of seven different disaccharides, richer in TriS disaccharides, and more structurally similar to heparin than any of the dual transfectants (Table 1). To our surprise, by correctly targeting HS3st1 and without introducing exogenous NDST2, it appeared that we may have increased the action of the endogenous CHO cell NDST1, GLCE, HS2st, and HS6sts. In addition, this observation is consistent with the results obtained using a mastocytoma cell line, where up-regulation of HS3st1 in a Furth murine mastocytoma cell line resulted in generation of AT-binding sites and an increase in TriS HS disaccharides (45, 46). These data suggest a

Downloaded from http://www.jbc.org/ at RENSSELAER POLYTECHNIC IN on December 30, 2013

TABLE 1

Quantification analysis of heparin/HS disaccharides by AMAC-LC/MS

HS was isolated from wild-type CHO-S, CHO-ndst2, Dual-10, Dual-29, and CHO-gt31 cell pellets. CHO-S cells were stably transfected with human NDST2 to form the CHO-ndst2 cell line, which was subsequently stably transfected with mouse HS3st1 to form the Dual-29 and Dual-10 cell lines. CHO-S cells stably transfected with Golgi-targeted mouse HS3st1 formed the CHO-gt31 cell line. Heparin was used as a positive control. The results represent the mean ± S.D. (n = 2–3 independent experiments). ND, not determined.

Sample	Heparin/HS							
	TriS	NS6S	NS2S	NS	2S6S	6S	2S	0S
	% mol							
CHO-S cell pellet (n = 2)	2.6 ± 3.7	ND	1.6 ± 2.3	12.7 ± 3.5	ND	2.7 ± 0.9	ND	80.4 ± 10.6
CHO-ndst2 cell pellet (n = 2)	1.3 ± 0.1	1.7 ± 0.4	16.5 ± 0.9	70.6 ± 1.8	ND	9.9 ± 0.4	ND	ND
Dual-10 cell pellet (n = 2)	0.7 ± 0.4	0.6 ± 0.7	10.1 ± 4.7	72.7 ± 11.2	ND	ND	ND	15.9 ± 17.7
Dual-29 cell pellet (n = 2)	2.8 ± 0.1	ND	5.1 ± 0.4	88.1 ± 2.5	ND	ND	ND	4.3 ± 4.3
CHO-gt31 cell pellet (n = 3)	9.7 ± 6.8	1.1 ± 0.1	6.3 ± 2.9	17.1 ± 2.0	ND	1.5 ± 0.1	2.7 ± 1.2	61.6 ± 8.0
CHO-gt31 spent medium (n = 2)	10.9 ± 6.4	1.7 ± 1.2	5.7 ± 1.2	14.0 ± 0.1	ND	1.8 ± 0.0	2.1 ± 1.2	63.8 ± 7.5
Heparin	75.3	10.4	5.1	2.3	0.8	3.2	1.8	1.1

previously unknown concerted interplay between the HS biosynthetic enzymes.

Heparin/HS and CS/DS biosynthesis begins with initiation of a tetrasaccharide linker on serine-rich residues in core proteins. The fate of the tetrasaccharide linker to form heparin/HS or CS/DS depends upon the addition of the next monosaccharide to the glucuronic acid residue. The addition of GalNAc initiates the polymerization of CS/DS (3). Polymerization of CS/DS is followed by modification of the nascent CS/DS chain, namely (*a*) epimerization of GlcUA to form IdoUA by action of GlcUA C5-epimerase and (*b*) sulfonation at positions 4 and 6 of GalNAc residues and at position 2 of GlcUA residues. CS/DS glycosaminoglycans are also found in CHO cells, and CHO cells express CS/DS sulfotransferases, as evidenced by CS/DS sulfonation patterns in adherent CHO cells (47–49). As heparin/HS and CS/DS share similar resources, including precursor molecules, uridine diphosphate sugars, and 3′-phosphoadenosine 5′-phosphosulfate (PAPS), our next question was how up-regulation of HS3st1 impacts CS/DS glycomics in CHO-gt31 cells (Fig. 4, *a* and *b*). To determine the effects of HS3st1 up-regulation on the CS/DS pathway, total GAGs were isolated from the cell pellet and purified. Total GAGs, heparin/HS, and CS/DS were isolated from the cell pellet and quantified by carbazole assays and AMAC/LC-MS (Table 2). In wild-type CHO-S cells, the primary GAGs were HS (3.33 μg/10^7 cells), followed by CS/DS (0.44 μg/10^7 cells). In CHO-gt31 cells, the amount of HS was 3.68 μg/10^7 cells, and that of CS/DS was 0.36 μg/10^7 cells. The ratios of heparin/HS and CS/DS isolated from cell pellets of CHO-S, CHO-ndst2, Dual-10, Dual-29, and CHO-gt31 cells were similar (n = 2) (Fig. 4*a*). The variability in the ratios of heparin/HS and CS/DS in CHO-gt31 cells was high as expected, as the CHO-gt31 cells were bulk stable pools. The CHO-gt31 cells were created by stably transfecting CHO-S cells with Golgi-targeted HS3st1 plasmid, resulting in a stable bulk pool expressing varied amounts of exogenous HS3st1. Stable transfection is the result of random integration of the expression vector in the daughter cell's chromosome and may impact other cellular processes directly or indirectly (36). The composition of CS/DS was determined by AMAC/LC-MS. The CS/DS composition of CHO-S cells was simple, containing only a 4-*O*-sulfo group (Fig. 4*b*). However, the CS/DS composition of CHO-gt31 cells included mainly 4S CS/DS disaccharides and increases in 0S, SB, and SE CS/DS disaccharides (Fig. 4*b*). The changes in CS/DS glycomics were interesting, as similar

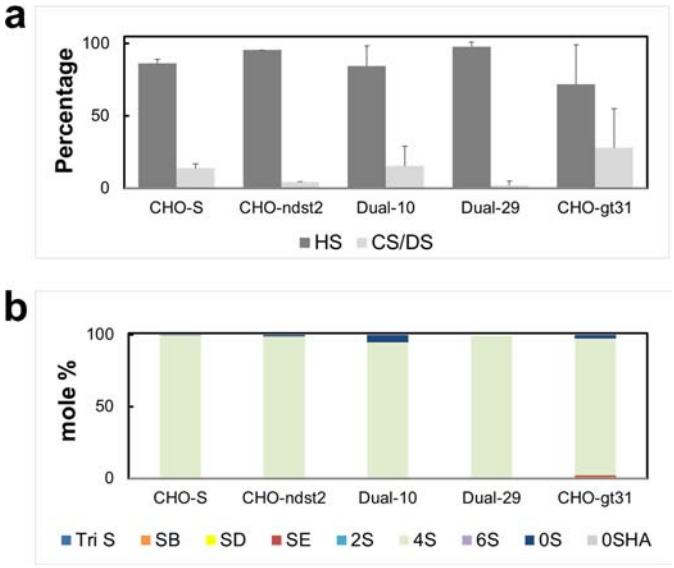

FIGURE 4. **CS/DS structural glycomics of CHO-S, CHO-ndst2, Dual-10, Dual-29, and CHO-gt31 cells.** *a*, ratio of HS and CS/DS from total GAGs isolated from cell pellets. Data represents the mean ± S.D. (n = 2). *b*, CS/DS disaccharide composition analysis.

TABLE 2

Amount of total GAG, heparin/HS, and CS/DS in cell pellets

GAG	CHO-S cells	CHO-gt31 cells
GAGs (μg/10^7 cells)	3.77	4.04
Heparin/HS (μg/10^7 cells)	3.33	3.68
CS/DS (μg/10^7 cells)	0.44	0.36

changes were not observed in the Dual-29 cell CS/DS composition; however, similar changes were observed in the CS/DS composition in a mastocytoma cell line overexpressing exogenous HS3st1 (45). These results further reiterate the complex interplay of biosynthetic enzymes in the biosynthetic pathway of proteoglycans in mammalian systems.

Heparin/HS and CS/DS proteoglycanomics is a non-template-driven process. The up-regulation of HS3st1 in CHO-S cells resulted in changes in proteoglycanomics in CHO-gt31 cells. In similar studies, the up-regulation of EXT1/2 glycosyltransferases, which have been associated with heparin/HS chain elongation (40), showed changes in the heparin/HS and CS/DS proteoglycanome in CHO-S cells, including increased binding affinity for FGF-2 (Fig. 5). In a parallel study, transient overexpression of HS2sts and HS6st1 in CHO-ndst2 cell lines showed a significant increase in the 2-*O*-sulfo and 6-*O*-sulfo

Downloaded from http://www.jbc.org/ at RENSSELAER POLYTECHNIC IN on December 30, 2013

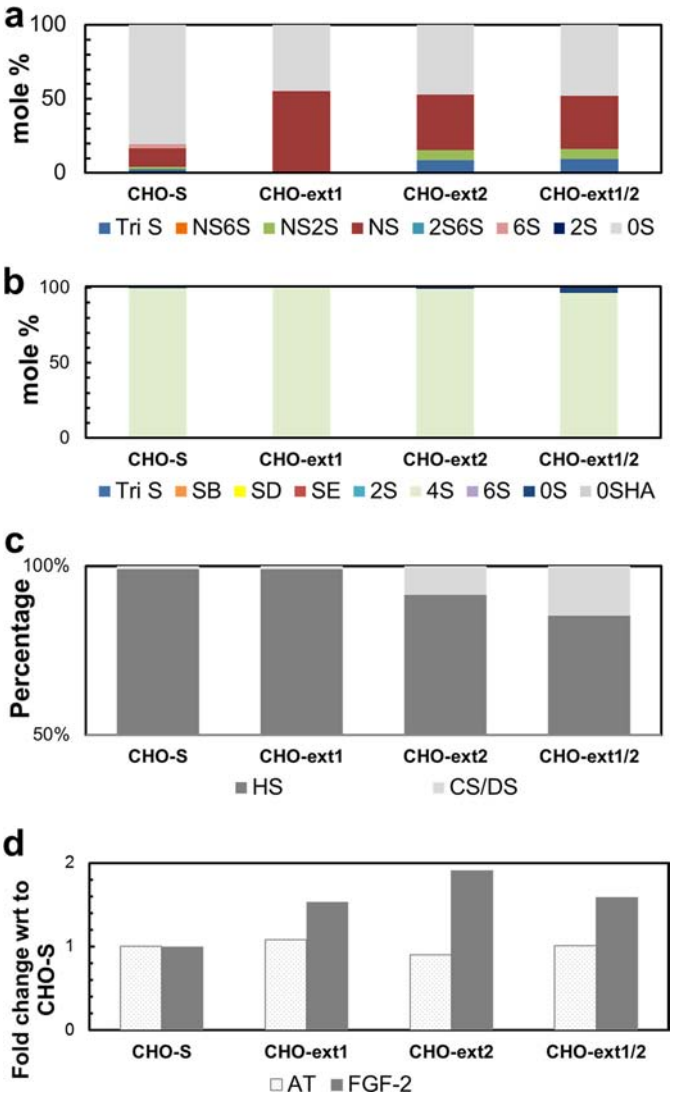

FIGURE 5. **Proteglycanomics (GAGs from the cell pellet) of wild-type CHO-S cells and CHO-S cells overexpressing EXT1, EXT2 and EXT1/2 biosynthetic enzymes.** *a*, HS GAGs were isolated from the cell pellet, and HS disaccharide composition was analyzed by AMAC/LC-MS. An increase in TriS HS disaccharides, suggestive of elevated action of *N*-, 2-*O*-, and 6-*O*-sulfotransferases, was observed in CHO-S cells overexpressing EXT2 (*CHO-ext2*) and EXT1 and EXT2 (*CHO-ext1/2*). *b*, CS/DS GAGs disaccharide analysis. An increase in 0S CS disaccharides was observed in CHO-S cells overexpressing EXT1 and EXT2. *c*, percentage of HS and CS/DS GAGs. An increase in CS/DS GAGs was seen in CHO-S cells overexpressing EXT1 and EXT2. *d*, normalized binding activity of AT and FGF-2 in wild-type, EXT1-overexpressing, EXT2-overexpressing, and EXT1/2-overexpressing CHO-S cells by flow cytometry ($n = 10000$ events). *wrt*, with respect to.

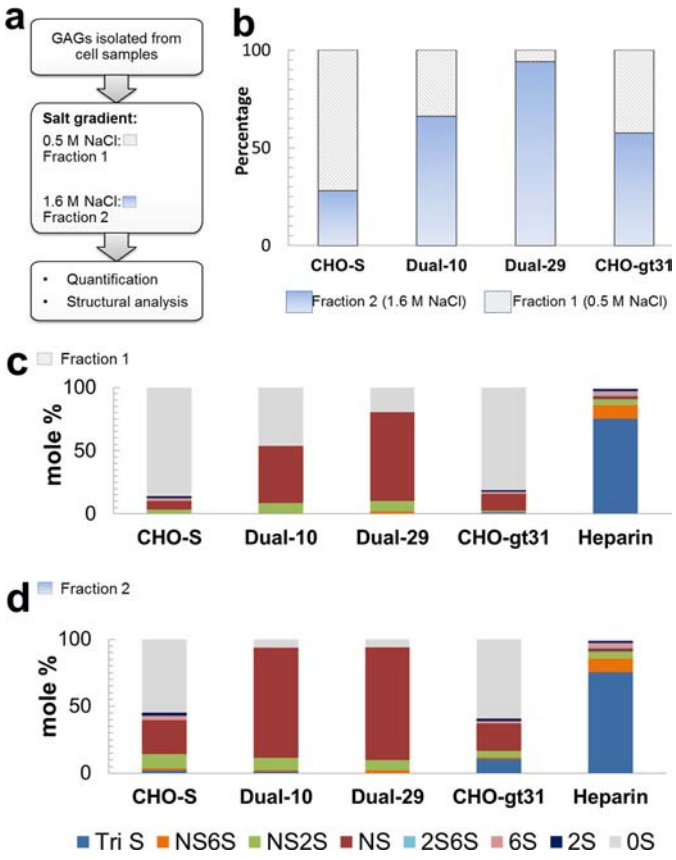

FIGURE 6. **Fractionation of GAGs by strong anion exchange chromatography demonstrates the existence of different populations of sulfated HS in wild-type and recombinant CHO cells.** The CS/DS GAGs were removed from the preparation before heparin/HS GAG quantification. *a*, experimental design showing that total GAGs were isolated from cell samples and subjected to a salt gradient. Fraction 1 (eluted at 0.5 M NaCl) contained mainly less sulfated HS GAGs, and Fraction 2 (eluted at 1.6 M NaCl) contained mainly highly sulfated heparin/HS GAGs. *b*, quantification of Fractions 1 and 2. *c*, disaccharide profile of fractionated GAGs from Fraction 1. *d*, disaccharide analysis of fractionated GAGs from Fraction 2. The composition of pharmaceutical heparin is shown in both *c* and *d* for comparison.

group-containing bioengineered HS and little or no changes in the CS/DS composition (data not shown). On the basis of the results obtained from the disaccharide analysis of bioengineered heparin/HS in this study, we hypothesize that heparin/HS biosynthetic enzymes may interact indirectly or directly to regulate the composition of heparin/HS and that bioengineering the heparin pathway in CHO cells would require controlled regulation of heparin/HS biosynthesis, including polymerization (glycosyltransferases) and modification processes. In addition, the levels of sulfation of GAGs depend upon the rate of synthesis, and in a parallel experiment (data not shown), we observed that the heparin/HS composition of GAGs isolated from spent media in CHO-S and Dual-29 cells varied depending on culture duration.

Fractionation of HS GAGs by Strong Anion Exchange Chromatography Demonstrates the Existence of Distinct Populations of Sulfated HS in Wild-type and Recombinant CHO Cells—Next, the HS isolated from wild-type CHO-S, Dual-10, Dual-29, and CHO-gt31 cell pellets was fractionated by ion exchange chromatography to remove less sulfated HS chains (released with low salt) to provide a better understanding of the HS sulfation level (Fig. 6*a*) (42). The CHO-S, Dual-10, Dual-29, and CHO-gt31 cell pellets contained two populations of HS GAG chains (Fig. 6*b*). The CHO-S cell pellet contained 72% less sulfated HS chains and 28% highly sulfated HS. The Dual-10 cell pellet, with low expression of NDST2 and HS3st1, contained 34% less sulfated HS chains and 66% highly sulfated HS. The Dual-29 cell pellet, with high expression of NDST2 and HS3st1, contained 6% less sulfated HS chains and 94% highly sulfated HS. Despite their high content of more highly sulfated HS chains (released with high salt), tetrasaccharide analysis of the fractionated HS from the Dual-29 and Dual-10 cell pellets did not demonstrate the presence of 3-*O*-sulfo groups. Moreover,

Downloaded from http://www.jbc.org/ at RENSSELAER POLYTECHNIC IN on December 30, 2013

a

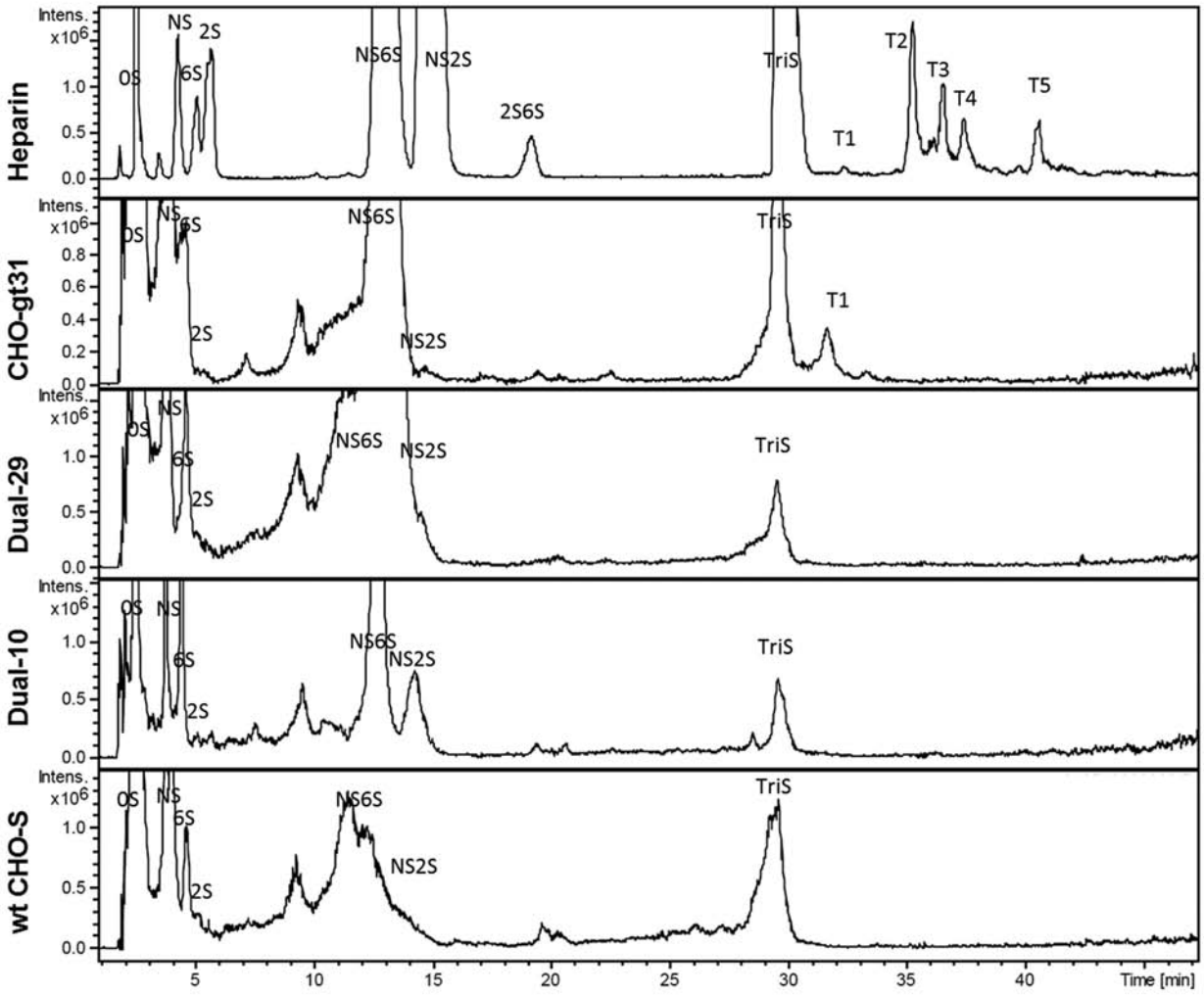

b

Fractions	m/z	Calculated Mol Mass	Theoretical Mol Mass	Sequence
T1	$[477.4]^{2-}$	956.8	956.1	ΔUA-GlcNAc6S-GlcA-GlcNS3S
T2	$[496.6]^{2-}$	994.4	994.0	ΔUA-GlcNS-GlcA-GlcNS3S6S
T3	$[496.6]^{2-}$	994.4	994.0	ΔUA-GlcNS6S-GlcA-GlcNS3S
T4	$[517.4]^{2-}$	1036.8	1036.0	ΔUA-GlcNAc6S-GlcA-GlcNS3S6S
T5	$[536.3]^{2-}$	1074.6	1074.0	ΔUA-GlcNS6S-GlcA-GlcNS3S6S

FIGURE 7. **Oligosaccharide mapping of bovine lung heparin and HS GAGS from CHO-gt31, Dual-29, Dual-10, and wild-type CHO-S cells by AMAC/LC-MS analysis.** *a*, tetrasaccharide structures in CHO-S, Dual-29, Dual-10, and CH-GT31 cell pellets are compared with bovine lung heparin. *b*, structures were assigned by MS analysis. The degree of sulfation of tetrasaccharide structures increased in successive tetrasaccharides, *i.e.* T1 < T2 < T3 < T4 < T5.

the major structure in the dual expression cell lines was not the TriS disaccharide found in heparin but the NS disaccharide (Fig. 2*b*). This suggests that the expression level of NDST2 may be too high, possibly overwhelming the actions of other enzymes. It has been hypothesized that NDST is involved in the termination of sulfonation in heparin/HS (28), and it may be that overexpression of NDST terminates the sulfonation of HS before the *O*-sulfotransferases can act on the HS chain. The GAGs from the CHO-gt31 cell pellet contained 42.5 ± 29% less sulfated HS chains and 57.5 ± 29% highly sulfated HS (mean ± S.D., where $n = 2$ independent bulk pool CHO-gt31 stable transfectants), suggesting that some HS GAG chains from CHO-gt31 cells were undersulfated.

Next, the composition of the fractionated heparin/HS from Dual-10, Dual-29, and CHO-gt31 cells was analyzed (Fig. 6, *c* and *d*). Fig. 6*c* shows the composition of the GAGs recovered by elution with 0.5 M NaCl (Fraction 1). Fig. 6*d* shows the composition of the GAGs recovered by elution with 1.6 M NaCl (Frac-

Downloaded from http://www.jbc.org/ at RENSSELAER POLYTECHNIC IN on December 30, 2013

TABLE 3

Quantification of the total amount of 3-*O*-sulfo group-containing oligosaccharides in total heparin/HS in bovine lung heparin and HS GAGs isolated from the cell pellets and media of wild-type CHO-S, Dual-29, and CHO-gt31 cells

The degree of sulfation of T1 < T2 < T3 < T4 < T5 increases is as follows: T1 = ΔUA-GlcNAc6S-GlcA-GlcNS3S, T2 = ΔUA-GlcNS-GlcA-GlcNS3S6S, T3 = ΔUA-GlcNS6S-GlcA-GlcNS3S, T4 = ΔUA-GlcNAc6S-GlcA-GlcNS3S6S, and T5 = ΔUA-GlcNS6S-GlcA-GlcNS3S6S. The results represent the mean ± S.D. (n = 2).

Sample	3-*O*-Sulfated oligosaccharide fraction					Total amount of 3-*O*-sulfated oligosaccharide fractions in total heparin/HS
	T1	T2	T3	T4	T5	
						%
Bovine lung heparin	+	+	+	+	+	4.00 ± 1.41
CHO cell pellet	−	−	−	−	−	
CHO spent medium	−	−	−	−	−	
Dual-29 cell pellet	−	−	−	−	−	
Dual-29 spent medium	−	−	−	−	−	
CHO-gt31 cell pellet	+	−	−	−	−	3.20 ± 0.57
CHO-gt31 spent medium	+	−	−	−	−	0.6

tion 2). As expected, GAGs recovered in Fraction 1 (Fig. 6*c*) had less sulfated HS GAGs compared with the highly sulfated HS GAGs recovered in Fraction 2 (Fig. 6*d*). The main GAG recovered from the CHO-S cell pellet in 0.5 M NaCl (Fraction 1) consisted mainly of less sulfated HS (Fig. 6*c*). The sulfated heparin/HS GAG from Fraction 2 of CHO-S cells was composed mainly of 0S, NS, and NS2S disaccharides (Fig. 6*d*). However, the HS from Dual-10 and Dual-29 cells consisted primarily of NS disaccharides (Fig. 6, *c* and *d*). The CHO-gt31 cells also contained two populations of HS GAGs. Notably, there was a significant increase in the TriS heparin/HS in Fraction 2. The failure of any of the engineered cell lines to show predominantly trisulfated GAGs might be the result of sulfate limitation in the media or limitation of the required biosynthetic enzymes, chaperones, or core proteins.

Role of HS3st1 Expression in Generation of the AT-binding Site in HS GAGs—Next, we turned our attention to the role of HS3st1 expression in the biosynthesis of the AT-binding site. When pharmaceutical heparins are treated with heparin lyase-2, as many as five tetrasaccharides are formed, with 3-*O*-sulfoglucosamine at their reducing ends (50). These correspond to a structural signature of the AT-binding site structural variants correlating with the anticoagulant activity of heparin (44). A tetrasaccharide analysis was performed on heparin lyase-2-treated HS from CHO-S, Dual-29, Dual-10, and CHO-gt31 cells and spent media. Only CHO-gt31 cells (3.2%) (Fig. 7) and spent media (0.6%) afforded HS with a heparin lyase-2-resistant tetrasaccharide of the structure ΔUA-GlcNAc6S-GlcUA-GlcNS3S, consistent with the action of HS3st1 creating an AT-binding site in HS from CHO-gt31 cells (Table 3). Based on biochemical studies and the crystal structure of the ternary complex of HS3st1 with PAPS and an HS oligosaccharide, HS3st1 has a known substrate specificity that indicates that it can act on GlcN(Ac/S)6(S/OH)-GlcUA-*GlcNS**3OH***(6S/OH)-IdoUA2S-GlcNS(6S/OH) (51), resulting in as many as the five structural variants of AT-binding sites observed in pharmaceutical heparins (44). Although CHO-gt31 cells and spent media contain an HS with a GlcNAc6S-GlcUA-*GlcNS**3S***6S-IdoUA2S-GlcNS(6S/OH) AT-binding site, these cells have only exogenous HS3st1; endogenous levels of NDST1, HS2st, GLCE, and HS6sts; and no detectable levels of NDST2 (38, 39). Thus, it is surprising that the overexpression of Golgi-targeted HS3st1 in CHO-S cells resulted in the formation of this AT-binding site.

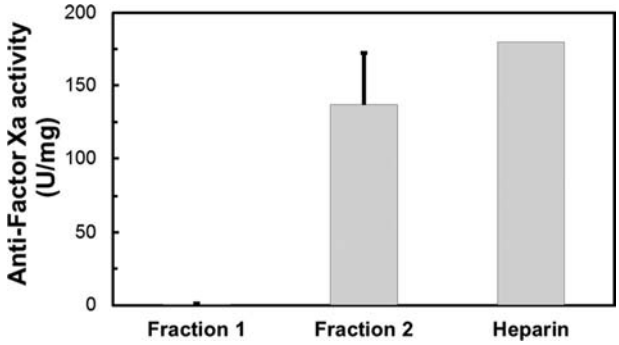

FIGURE 8. **Anti-factor Xa assay.** Bioengineered HS from CHO-gt31 cells was fractionated, and anti-factor Xa activity was assessed with heparin as the control. Values are the mean ± S.E. (n = 3).

Biological Characterization of Bioengineered Heparin/HS from CHO-gt31 Cells—CHO-gt31 cells produce an HS containing a GlcNAc6S-GlcUA-GlcNS3S6S-IdoUA2S-GlcNS(6S/OH) AT-binding site, comprising 4% of the total HS isolated from the cell pellet (Table 3). The anticoagulant activity was assessed using an anti-factor Xa chromogenic assay, which determines the ability of the GAG to bind to and mediate the AT inactivation of factor Xa. The activation of AT by heparin relies on a bridging mechanism for thrombin and is sensitive only to conformational change (allosteric) for factors Xa and IXa. Pharmaceutical heparin from different sources has differential amounts of AT-binding sites and exhibits some differences in anti-factor Xa activity (44). The highly *N*-sulfated HS from Dual-29 cells does not contain any 3-*O*-sulfo groups as determined by tetrasaccharide analysis and thus does not contain AT-binding sites and shows a relatively low anti-factor Xa activity (2–4 units/mg) (39). The wild-type CHO-S cell unsulfated HS similarly shows no evidence of AT-binding sites and an anti-factor Xa activity of 0.2 units/mg. The HS isolated from CHO-gt31 cells was fractionated to obtain Fraction 1 (containing less sulfated HS chains) and Fraction 2 (containing highly sulfated heparin/HS-like GAG). The anti-factor Xa activity of the two fractions was measured (Fig. 8). Fraction 1 had an anti-factor Xa activity of 0.6 ± 0.5 units/mg, whereas Fraction 2 showed an anti-factor Xa activity of 137 ± 36 units/mg. The anti-factor Xa activity of pharmaceutical heparin is >180 units/mg (44).

Conclusions—HS3st transfers a sulfo group from PAPS to the 3-OH of *N*-sulfoglucosamine to form 3-*O*-sulfo-*N*-sulfoglucosamine-containing (GlcNS3S±6S) HS chains. *In vivo*, HS can be

Downloaded from http://www.jbc.org/ at RENSSELAER POLYTECHNIC IN on December 30, 2013

modified by seven different HS3st isoforms that exhibit different physiological and pathophysiological functions (52, 53). HS3st1 has been shown to be critical in forming the AT-binding site on anticoagulant HS and heparin. In previous studies, in an effort to bioengineer heparin in CHO cells, two critical enzymes, NDST2 and HS3st1, were stably overexpressed in suspension-adapted CHO-S cells, resulting in 40 stable dual clones (39). Characterization of two dual clones (Dual-3 and Dual-29) showed that the bioengineered HS from these cells was highly *N*-sulfated but showed only modest increases in anti-factor Xa activity. These results suggest a low activity of HS3st1 compared with its expression level and imply either that HS3st1 is inactive or there is a limitation in HS3st1 substrates or chaperones. These questions led us to probe factors that might impact HS3st1 activity in bioengineered CHO-S cells.

The results from this study confirmed the activity of HS3st1 in transfected CHO-S cells (bioengineered CHO-gt31 cells). HS from bioengineered CHO-S cells with Golgi-targeted HS3st1 (CHO-gt31 cells) showed the presence of a tetrasaccharide that is a structural signature of the AT-binding site and demonstrated the stable overexpression of Golgi-targeted HS3st1 in these cells. It is still unclear, however, why only a single type of AT-binding site was observed instead of the multiple AT-binding sites characterized from animal-sourced pharmaceutical heparins. One might speculate that the controlled expression of other modification enzymes in CHO-S cells, specifically NDST2, HS6sts, GLCE, and HS2st, will be needed to produce an HS with a heparin-like disaccharide composition having multiple AT-binding sites. Moreover, this study showed that overexpression of *N*-sulfotransferase reduced the action of HS3st1 in CHO-S cells (*e.g.* in bioengineered dual clones), indicating that controlled expression of HS enzymes will be crucial for obtaining heparin-like GAGs from CHO cells. In addition, HS3st1 expression in CHO-gt31 cells also resulted in an increase in TriS HS disaccharides in the HS isolated from the cell pellet. TriS HS disaccharide formation is a result of the action of *N*-, 2-*O*-, and 6-*O*-sulfotransferases, indicating that overexpression of Golgi-targeted HS3st1 in CHO-S cells can increase the action of other sulfotransferases.

Heparin/HS biosynthesis involves a non-template-driven process. The EXT glycosyltransferases are involved in HS chain elongation during heparin/HS biosynthesis (40), affecting NDST activity (54), which in turn impacts the CHO-S proteoglycanome. The HS3st1 heparin/HS biosynthetic enzyme has been postulated to work in the final step of the heparin/HS biosynthetic pathway (4, 39); however, the current study suggests a previously unknown interplay between HS3st1 and upstream HS biosynthetic enzymes. In conclusion, it appears that the production of biopharmaceutical heparin in CHO cells will require the controlled regulation of heparin/HS polymerization (glycosyltransferases) and modification processes.

Acknowledgment—We thank Dr. Lena Kjellén for the gracious gift of the EXT1, EXT2, and dual EXT1/2 expression vectors.

REFERENCES

1. Dreyfuss, J. L., Regatieri, C. V., Jarrouge, T. R., Cavalheiro, R. P., Sampaio, L. O., and Nader, H. B. (2009) Heparan sulfate proteoglycans: structure, protein interactions and cell signaling. *An. Academ. Bras. Cienc.* **81,** 409–429
2. Liu, H., Zhang, Z., and Linhardt, R. J. (2009) Lessons learned from the contamination of heparin. *Nat. Prod. Rep.* **26,** 313–321
3. Carlsson, P., and Kjellén, L. (2012) Heparin biosynthesis. *Handb. Exp. Pharmacol.* **207,** 23–41
4. Esko, J. D., and Lindahl, U. (2001) Molecular diversity of heparan sulfate. *J. Clin. Invest.* **108,** 169–173
5. Esko, J. D., and Zhang, L. (1996) Influence of core protein sequence on glycosaminoglycan assembly. *Curr. Opin. Struct. Biol.* **6,** 663–670
6. Gulberti, S., Lattard, V., Fondeur, M., Jacquinet, J. C., Mulliert, G., Netter, P., Magdalou, J., Ouzzine, M., and Fournel-Gigleux, S. (2005) Phosphorylation and sulfation of oligosaccharide substrates critically influence the activity of human β1,4-galactosyltransferase 7 (GalT-I) and β1,3-glucuronosyltransferase I (GlcAT-I) involved in the biosynthesis of the glycosaminoglycan-protein linkage region of proteoglycans. *J. Biol. Chem.* **280,** 1417–1425
7. Tone, Y., Pedersen, L. C., Yamamoto, T., Izumikawa, T., Kitagawa, H., Nishihara, J., Tamura, J., Negishi, M., and Sugahara, K. (2008) 2-*O*-Phosphorylation of xylose and 6-*O*-sulfation of galactose in the protein linkage region of glycosaminoglycans influence the glucuronyltransferase-I activity involved in the linkage region synthesis. *J. Biol. Chem.* **283,** 16801–16807
8. Duelli, A., Rönnberg, E., Waern, I., Ringvall, M., Kolset, S. O., and Pejler, G. (2009) Mast cell differentiation and activation is closely linked to expression of genes coding for the serglycin proteoglycan core protein and a distinct set of chondroitin sulfate and heparin sulfotransferases. *J. Immunol.* **183,** 7073–7083
9. Kramer, K. L., and Yost, H. J. (2003) Heparan sulfate core proteins in cell-cell signaling. *Annu. Rev. Genet.* **37,** 461–484
10. Wang, Z., Ly, M., Zhang, F., Zhong, W., Suen, A., Hickey, A. M., Dordick, J. S., and Linhardt, R. J. (2010) *E. coli* K5 fermentation and the preparation of heparosan, a bioengineered heparin precursor. *Biotechnol. Bioeng.* **107,** 964–973
11. Grobe, K., Ledin, J., Ringvall, M., Holmborn, K., Forsberg, E., Esko, J. D., and Kjellén, L. (2002) Heparan sulfate and development: differential roles of the *N*-acetylglucosamine *N*-deacetylase/*N*-sulfotransferase isozymes. *Biochim. Biophys. Acta* **1573,** 209–215
12. Hashimoto, Y., Orellana, A., Gil, G., and Hirschberg, C. B. (1992) Molecular cloning and expression of rat liver *N*-heparan sulfate sulfotransferase. *J. Biol. Chem.* **267,** 15744–15750
13. Aikawa, J., and Esko, J. D. (1999) Molecular cloning and expression of a third member of the heparan sulfate/heparin GlcNAc *N*-deacetylase/*N*-sulfotransferase family. *J. Biol. Chem.* **274,** 2690–2695
14. Aikawa, J., Grobe, K., Tsujimoto, M., and Esko, J. D. (2001) Multiple isozymes of heparan sulfate/heparin GlcNAc *N*-deacetylase/GlcN *N*-sulfotransferase. Structure and activity of the fourth member, NDST4. *J. Biol. Chem.* **276,** 5876–5882
15. Eriksson, I., Sandbäck, D., Ek, B., Lindahl, U., and Kjellén, L. (1994) cDNA cloning and sequencing of mouse mastocytoma glucosaminyl *N*-deacetylase/*N*-sulfotransferase, an enzyme involved in the biosynthesis of heparin. *J. Biol. Chem.* **269,** 10438–10443
16. Kusche-Gullberg, M., Eriksson, I., Pikas, D. S., and Kjellén, L. (1998) Identification and expression in mouse of two heparan sulfate glucosaminyl *N*-deacetylase/*N*-sulfotransferase genes. *J. Biol. Chem.* **273,** 11902–11907
17. Orellana, A., Hirschberg, C. B., Wei, Z., Swiedler, S. J., and Ishihara, M. (1994) Molecular cloning and expression of a glycosaminoglycan *N*-acetylglucosaminyl *N*-deacetylase/*N*-sulfotransferase from a heparin-producing cell line. *J. Biol. Chem.* **269,** 2270–2276
18. Cheung, W. F., Eriksson, I., Kusche-Gullberg, M., Lindhal, U., and Kjellén, L. (1996) Expression of the mouse mastocytoma glucosaminyl *N*-deacetylase/*N*-sulfotransferase in human kidney 293 cells results in increased *N*-sulfation of heparan sulfate. *Biochemistry* **35,** 5250–5256
19. Jacobsson, I., Lindahl, U., Jensen, J. W., Rodén, L., Prihar, H., and Feingold, D. S. (1984) Biosynthesis of heparin. Substrate specificity of heparosan *N*-sulfate D-glucuronosyl 5-epimerase. *J. Biol. Chem.* **259,** 1056–1063
20. Rong, J., Habuchi, H., Kimata, K., Lindahl, U., and Kusche-Gullberg, M. (2001) Substrate specificity of the heparan sulfate hexuronic acid 2-*O*-

Downloaded from http://www.jbc.org/ at RENSSELAER POLYTECHNIC IN on December 30, 2013

sulfotransferase, *Biochemistry* **40,** 5548–5555
21. Habuchi, H., Nagai, N., Sugaya, N., Atsumi, F., Stevens, R. L., and Kimata, K. (2007) Mice deficient in heparan sulfate 6-*O*-sulfotransferase-1 exhibit defective heparan sulfate biosynthesis, abnormal placentation, and late embryonic lethality. *J. Biol. Chem.* **282,** 15578–15588
22. Habuchi, H., Tanaka, M., Habuchi, O., Yoshida, K., Suzuki, H., Ban, K., and Kimata, K. (2000) The occurrence of three isoforms of heparan sulfate 6-*O*-sulfotransferase having different specificities for hexuronic acid adjacent to the targeted *N*-sulfoglucosamine. *J. Biol. Chem.* **275,** 2859–2868
23. Jemth, P., Smeds, E., Do, A. T., Habuchi, H., Kimata, K., Lindahl, U., and Kusche-Gullberg, M. (2003) Oligosaccharide library-based assessment of heparan sulfate 6-*O*-sulfotransferase substrate specificity. *J. Biol. Chem.* **278,** 24371–24376
24. Smeds, E., Habuchi, H., Do, A. T., Hjertson, E., Grundberg, H., Kimata, K., Lindahl, U., and Kusche-Gullberg, M. (2003) Substrate specificities of mouse heparan sulphate glucosaminyl 6-*O*-sulphotransferases. *Biochem. J.* **372,** 371–380
25. Girardin, E. P., Hajmohammadi, S., Birmele, B., Helisch, A., Shworak, N. W., and de Agostini, A. I. (2005) Synthesis of anticoagulantly active heparan sulfate proteoglycans by glomerular epithelial cells involves multiple 3-*O*-sulfotransferase isoforms and a limiting precursor pool. *J. Biol. Chem.* **280,** 38059–38070
26. Liu, J., Shworak, N. W., Sinaÿ, P., Schwartz, J. J., Zhang, L., Fritze, L. M., and Rosenberg, R. D. (1999) Expression of heparan sulfate D-glucosaminyl 3-*O*-sulfotransferase isoforms reveals novel substrate specificities. *J. Biol. Chem.* **274,** 5185–5192
27. Shworak, N. W., Liu, J., Petros, L. M., Zhang, L., Kobayashi, M., Copeland, N. G., Jenkins, N. A., and Rosenberg, R. D. (1999) Multiple isoforms of heparan sulfate D-glucosaminyl 3-*O*-sulfotransferase. Isolation, characterization, and expression of human cDNAs and identification of distinct genomic loci. *J. Biol. Chem.* **274,** 5170–5184
28. Esko, J. D., and Selleck, S. B. (2002) Order out of chaos: assembly of ligand binding sites in heparan sulfate. *Annu. Rev. Biochem.* **71,** 435–471
29. Humphries, D. E., Wong, G. W., Friend, D. S., Gurish, M. F., Qiu, W. T., Huang, C., Sharpe, A. H., and Stevens, R. L. (1999) Heparin is essential for the storage of specific granule proteases in mast cells. *Nature* **400,** 769–772
30. Forsberg, E., Pejler, G., Ringvall, M., Lunderius, C., Tomasini-Johansson, B., Kusche-Gullberg, M., Eriksson, I., Ledin, J., Hellman, L., and Kjellén, L. (1999) Abnormal mast cells in mice deficient in a heparin-synthesizing enzyme. *Nature* **400,** 773–776
31. Feyerabend, T. B., Li, J. P., Lindahl, U., and Rodewald, H. R. (2006) Heparan sulfate C5-epimerase is essential for heparin biosynthesis in mast cells. *Nat. Chem. Biol.* **2,** 195–196
32. Anower-E-Khuda M. F., Habuchi, H., Nagai, N., Habuchi, O., Yokochi, T., and Kimata, K. (2013) Heparan sulfate 6-*O*-sulfotransferase isoform-dependent regulatory effects of heparin on the activities of various proteases in mast cells and the biosynthesis of 6-*O*-sulfated heparin. *J. Biol. Chem.* **288,** 3705–7317
33. Zhang, L., Beeler, D. L., Lawrence, R., Lech, M., Liu, J., Davis, J. C., Shriver, Z., Sasisekharan, R., and Rosenberg, R. D. (2001) 6-*O*-Sulfotransferase-1 represents a critical enzyme in the anticoagulant heparan sulfate biosynthetic pathway. *J. Biol. Chem.* **276,** 42311–42321
34. Shworak, N. W., Kobayashi, T., de Agostini, A., and Smits, N. C. (2010) Anticoagulant heparan sulfate to not clot– or not? *Prog. Mol. Biol. Transl. Sci.* **93,** 153–178
35. Shworak, N. W., HajMohammadi, S., de Agostini, A. I., and Rosenberg, R. D. (2002) Mice deficient in heparan sulfate 3-*O*-sulfotransferase-1: normal hemostasis with unexpected perinatal phenotypes. *Glycoconj. J.* **19,** 355–361
36. Datta, P., Linhardt, R. J., and Sharfstein, S. T. (2013) An 'omics approach towards CHO cell engineering. *Biotechnol. Bioeng.* **110,** 1255–1271
37. Zhang, L., Lawrence, R., Frazier, B. A., and Esko, J. D. (2006) CHO glycosylation mutants: proteoglycans. *Methods Enzymol.* **416,** 205–221
38. Xu, X., Nagarajan, H., Lewis, N. E., Pan, S., Cai, Z., Liu, X., Chen, W., Xie, M., Wang, W., Hammond, S., Andersen, M. R., Neff, N., Passarelli, B., Koh, W., Fan, H. C., Wang, J., Gui, Y., Lee, K. H., Betenbaugh, M. J., Quake, S. R., Famili, I., Palsson, B. O., and Wang, J. (2011) The genomic sequence of the Chinese hamster ovary (CHO)-K1 cell line. *Nat. Biotechnol.* **29,** 735–741
39. Baik, J. Y., Gasimli, L., Yang, B., Datta, P., Zhang, F., Glass, C. A., Esko, J. D., Linhardt, R. J., and Sharfstein, S. T. (2012) Metabolic engineering of Chinese hamster ovary cells: towards a bioengineered heparin. *Metab. Eng.* **14,** 81–90
40. Busse, M., Feta, A., Presto, J., Wilén, M., Grønning, M., Kjellén, L., and Kusche-Gullberg, M. (2007) Contribution of EXT1, EXT2, and EXTL3 to heparan sulfate chain elongation. *J. Biol. Chem.* **282,** 32802–32810
41. Yang, B., Chang, Y., Weyers, A. M., Sterner, E., and Linhardt, R. J. (2012) Disaccharide analysis of glycosaminoglycan mixtures by ultra-high-performance liquid chromatography-mass spectrometry. *J. Chromatogr. A* **1225,** 91–98
42. Zhao, X., Yang, B., Linkens, K., Datta, P., Onishi, A., Zhang, F., and Linhardt, R. J. (2013) Microscale separation of heparosan, heparan sulfate, and heparin. *Anal. Biochem.* **434,** 215–217
43. Zhang, F., Yang, B., Ly, M., Solakyildirim, K., Xiao, Z., Wang, Z., Beaudet, J. M., Torelli, A. Y., Dordick, J. S., and Linhardt, R. J. (2011) Structural characterization of heparins from different commercial sources. *Anal. Bioanal. Chem.* **401,** 2793–2803
44. Fu, L., Li, G., Yang, B., Onishi, A., Li, L., Sun, P., Zhang, F., and Linhardt, R. J. (2013) Structural characterization of pharmaceutical heparins prepared from different animal tissues. *J. Pharm. Sci.* **102,** 1447–1457
45. Datta, P. (2013) *Cell Engineering and Modulation of Metabolic Pathways in Mammalian Cells for the Production of Glycoprotein and Proteoglycan Based Pharmaceuticals*. Doctoral thesis, Rensselaer Polytechnic Institute
46. Montgomery, R. I., Lidholt, K., Flay, N. W., Liang, J., Vertel, B., Lindahl, U., and Esko, J. D. (1992) Stable heparin-producing cell lines derived from the Furth murine mastocytoma. *Proc. Natl. Acad. Sci. U.S.A.* **89,** 11327–11331
47. Esko, J. D., Weinke, J. L., Taylor, W. H., Ekborg, G., Rodén, L., Anantharamaiah, G., and Gawish, A. (1987) Inhibition of chondroitin and heparan sulfate biosynthesis in Chinese hamster ovary cell mutants defective in galactosyltransferase I. *J. Biol. Chem.* **262,** 12189–12195
48. Esko, J. D., Stewart, T. E., and Taylor, W. H. (1985) Animal cell mutants defective in glycosaminoglycan biosynthesis. *Proc. Natl. Acad. Sci. U.S.A.* **82,** 3197–3201
49. Cuellar, K., Chuong, H., Hubbell, S. M., and Hinsdale, M. E. (2007) Biosynthesis of chondroitin and heparan sulfate in Chinese hamster ovary cells depends on xylosyltransferase II. *J. Biol. Chem.* **282,** 5195–5200
50. Zhao, W., Garron, M. L., Yang, B., Xiao, Z., Esko, J. D., Cygler, M., and Linhardt, R. J. (2011) Asparagine 405 of heparin lyase II prevents the cleavage of glycosidic linkages proximate to a 3-*O*-sulfoglucosamine residue. *FEBS Lett.* **585,** 2461–2466
51. Moon, A. F., Xu, Y., Woody, S. M., Krahn, J. M., Linhardt, R. J., Liu, J., and Pedersen, L. C. (2012) Dissecting the substrate recognition of 3-*O*-sulfotransferase for the biosynthesis of anticoagulant heparin. *Proc. Natl. Acad. Sci. U.S.A.* **109,** 5265–5270
52. Chen, J., and Liu, J. (2005) Characterization of the structure of antithrombin-binding heparan sulfate generated by heparan sulfate 3-*O*-sulfotransferase 5. *Biochim. Biophys. Acta* **1725,** 190–200
53. Zhang, L., Lawrence, R., Schwartz, J. J., Bai, X., Wei, G., Esko, J. D., and Rosenberg, R. D. (2001) The effect of precursor structures on the action of glucosaminyl 3-*O*-sulfotransferase-1 and the biosynthesis of anticoagulant heparan sulfate. *J. Biol. Chem.* **276,** 28806–28813
54. Presto, J., Thuveson, M., Carlsson, P., Busse, M., Wilén, M., Eriksson, I., Kusche-Gullberg, M., and Kjellén, L. (2008) Heparan sulfate biosynthesis enzymes EXT1 and EXT2 affect NDST1 expression and heparan sulfate sulfation. *Proc. Natl. Acad. Sci. U.S.A.* **105,** 4751–4756

Downloaded from http://www.jbc.org/ at RENSSELAER POLYTECHNIC IN on December 30, 2013